Received: 18 April 2019 | Revised: 12 August 2019 | Accepted: 25 August 2019

DOI: 10.1002/humu.23904

Human Mutation HGVS HUMAN GENOME VARIATION SOCIETY WILEY

RESEARCH ARTICLE

A rare heterozygous *TREM2* coding variant identified in familial clustering of dementia affects an intrinsically disordered protein region and function of TREM2

Meliha Karsak[1*] | Konstantin Glebov[2*] | Marina Scheffold[1,3] | Thomas Bajaj[4] | Amit Kawalia[4] | Ilker Karaca[5] | Sebastian Rading[1] | Johannes Kornhuber[6] | Oliver Peters[7] | Monica Diez-Fairen[8,9] | Lutz Frölich[10] | Michael Hüll[11] | Jens Wiltfang[12,13] | Martin Scherer[14] | Steffi Riedel-Heller[15] | Anja Schneider[5,16] | Michael T. Heneka[5,16,17] | Klaus Fliessbach[5] | Ahmed Sharaf[1] | Holger Thiele[18] | Martina Lennarz[19] | Frank Jessen[16,20] | Wolfgang Maier[5,16] | Christian Kubisch[21] | Zoya Ignatova[22] | Peter Nürnberg[18,23] | Pau Pastor[8,9] | Jochen Walter[2] | Alfredo Ramirez[4,5]

[1]Center for Molecular Neurobiology (ZMNH), University Medical Center Hamburg-Eppendorf (UKE), Hamburg, Germany

[2]Department of Neurology, University of Bonn, Bonn, Germany

[3]Institute of Pharmacology and Toxicology, University of Ulm, Ulm, Germany

[4]Division of Neurogenetics and Molecular Psychiatry, Department of Psychiatry and Psychotherapy, Medical Faculty, University of Cologne, Cologne, Germany

[5]Department of Neurodegenerative Diseases and Geriatric Psychiatry, University of Bonn, Bonn, Germany

[6]Department of Psychiatry and Psychotherapy, Universitätsklinikum Erlangen and Friedrich-Alexander Universität Erlangen-Nürnberg, Erlangen, Germany

[7]Department of Psychiatry, Charité University Medicine, Berlin, Germany

[8]Department of Neurology, Memory and Movement Disorders Units, University Hospital Mutua de Terrassa, Terrassa, Barcelona, Spain

[9]Fundació Docència i Recerca Mútua Terrassa, University Hospital Mútua de Terrassa, Terrassa, Barcelona, Spain

[10]Department of Geriatric Psychiatry, Central Institute of Mental Health, Medical Faculty Mannheim, University of Heidelberg, Mannheim, Germany

[11]Center for Psychiatry, Clinic for Geriatric Psychiatry and Psychotherapy Emmendingen and Department of Psychiatry and Psychotherapy, University of Freiburg, Freiburg, Germany

[12]Department of Psychiatry and Psychotherapy, University Medical Center Göttingen, Göttingen, Germany

[13]German Center for Neurodegenerative Diseases (DZNE), Göttingen, Germany

[14]Department of Primary Medical Care, University Medical Center Hamburg-Eppendorf, Hamburg, Germany

[15]Institute of Social Medicine, Occupational Health and Public Health, University of Leipzig, Leipzig, Germany

[16]German Center for Neurodegenerative Diseases (DZNE), Bonn, Germany

[17]Division of Infectious Diseases and Immunology, Department of Medicine, University of Massachusetts Medical School, Worcester, Massachusetts

[18]Cologne Center for Genomics (CCG), University of Cologne, Cologne, Germany

[19]Department of Psychiatry and Psychotherapy, University of Bonn, Bonn, Germany

[20]Department of Psychiatry and Psychotherapy, Medical Faculty, University of Cologne, Cologne, Germany

[21]Institute of Human Genetics, University Medical Center Hamburg-Eppendorf, Hamburg, Germany

[22]Institute for Biochemistry and Molecular Biology, University of Hamburg, Hamburg, Germany

[23]Center for Molecular Medicine Cologne (CMMC), University of Cologne, Cologne, Germany

*Meliha Karsak and Konstantin Glebov contributed equally to this study.

Correspondence
Jochen Walter, Department of Neurology–Molecular Cell Biology, University of Bonn Medical Center, Sigmund Freud Str. 25 to Venusberg-Campus 1, 53127 Bonn, Germany.
Email: jochen.walter@ukbonn.de

Alfredo Ramirez, Division of Neurogenetics and Molecular Psychiatry, Department of Psychiatry and Psychotherapy, University of Cologne, Kerpener Str. 62, 50931 Cologne, Germany.
Email: alfredo.ramirez@uk-koeln.de

Funding information
Deutsche Forschungsgemeinschaft, Grant/Award Number: WA1477/6-2; Innovative Medicines Initiative 2 Joint Undertaking, Grant/Award Number: 115976; Bundesministerium für Bildung und Forschung, Grant/Award Numbers: 01ET1006B, 01GI0102, 01GI0420, 01GI0422, 01GI0423, 01GI0429, 01GI0431, 01GI0433, 01GI0434, 01GI0710, 01GI0711, 01GI0712, 01GI0713, 01GI0714, 01GI0715, 01GI0716; Alzheimer Forschung Initiative, Grant/Award Number: 16019

Abstract

Rare coding variants in the triggering receptor expressed on myeloid cells-2 (*TREM2*) gene have been associated with Alzheimer disease (AD) and homozygous *TREM2* loss-of-function variants have been reported in families with monogenic frontotemporal-like dementia with/without bone abnormalities. In a whole-exome sequencing study of a family with probable AD-type dementia without pathogenic variants in known autosomal dominant dementia disease genes and negative for the apolipoprotein E (*APOE*) ε4 allele, we identified an extremely rare *TREM2* coding variant, that is, a glycine-to-tryptophan substitution at amino acid position 145 (NM_018965.3:c.433G>T/p.[Gly145Trp]). This alteration is found in only 1 of 251,150 control alleles in gnomAD. It was present in both severely affected as well as in another putatively affected and one 61 years old as yet unaffected family member suggesting incomplete penetrance and/or a variable age of onset. Gly145 maps to an intrinsically disordered region (IDR) of TREM2 between the immunoglobulin-like and transmembrane domain. Subsequent cellular studies showed that the variant led to IDR shortening and structural changes of the mutant protein resulting in an impairment of cellular responses upon receptor activation. Our results, suggest that a p.(Gly145Trp)-induced structural disturbance and functional impairment of TREM2 may contribute to the pathogenesis of an AD-like form of dementia.

KEYWORDS
Alzheimer disease, conformation, dementia, intrinsically disordered region, TREM2

1 | INTRODUCTION

Alzheimer disease (AD) is a multifactorial disorder characterized by progressive and irreversible neurodegeneration, which inexorably leads to dementia. As with most multifactorial disorders, susceptibility to AD results from complex interactions of genetic, epigenetic, and environmental factors. The estimated heritability of sporadic AD is 60–80% (Gatz et al., 2006). Since 2009, a growing number of common and rare genetic risk variants for AD (with minor allele frequencies [MAF] of > 5% and < 1%, respectively), besides *APOE*-ε4, have been identified by genome-wide association studies and next-generation sequencing approaches. While common variants usually have small to modest effect

sizes, the effect sizes observed for rare coding variants are often larger and in some instances exert a similar effect as *APOE-ε4*. Several rare coding variants have been described as susceptibility genes for AD, including alterations in *TREM2*, *ABCA7* (ATP binding cassette subfamily A member 7), *SORL1* (sortilin related receptor 1), *PLCG2* (phospholipase C gamma 2), and *ABI3* (ABI family member 3). Among them, the rare coding variant p.(Arg47His) in *TREM2* confers a three-fold increased risk for sporadic AD (Lill et al., 2015).

TREM2 is a type I membrane protein primarily expressed by microglial cells in the brain (Kiialainen, Hovanes, Paloneva, Kopra, & Peltonen, 2005). The protein lacks an intracellular signaling motif and functions by interacting with its coreceptor DAP12 (DNAX-activating protein of 12 kDa), also known as TYROBP (TYRO protein tyrosine kinase-binding protein), in microglial signal transduction (Ulland & Colonna, 2018; Villegas-Llerena, Phillips, Garcia-Reitboeck, Hardy, & Pocock, 2016; Walter, 2016). Both proteins form a plasma membrane-localized immune receptor complex (Wunderlich et al., 2013). TREM2 function has been linked to ApoE and loss of TREM2 has been suggested to lead to deficits in lipid sensing important for microglial activation and innate immune responses (Krasemann et al., 2017; Poliani et al., 2015; Shi & Holtzman, 2018; Yeh, Hansen, & Sheng, 2017). Moreover, TREM2–DAP12 is also involved in the recognition of membrane debris and amyloid deposits resulting in activation and proliferation of microglia.

In addition to *TREM2* susceptibility coding variants in AD, biallelic variants in *TREM2* have been reported in families with a rare autosomal recessive disease called polycystic lipomembranous osteodysplasia with sclerosing leukoencephalopathy (PLOSL, also known as Nasu–Hakola disease; Paloneva et al., 2003). This condition is characterized by early onset progressive dementia and bone cysts.

In addition, biallelic *TREM2* variants were also identified in families affected by frontotemporal (FTD)-like dementia without bone cysts (Guerreiro et al., 2013). Of note, the majority of *TREM2* variants that are linked to aforementioned monogenic neurodegenerative diseases, including p.(Arg47His), are located in exon 2 encoding the highly conserved extracellular immunoglobulin (Ig)-like domain. This region contains the ligand-binding domain of TREM2 and those rare variants are supposed to interfere with subcellular transport and ligand–receptor interaction, hence decreasing overall TREM2 signaling activity. In most cases, however, rare variants do not reach the level of penetrance seen in variants associated with monogenic forms of AD (Karch & Goate, 2015). Furthermore, with the exception of p.(Arg47His) and p.(Arg62His), a possible association of rare coding variants in *TREM2* with AD can often not be proven due to their low MAF, rendering their classification into pathogenic and nonpathogenic alterations difficult (Jin et al., 2014). Therefore, the analyses of families with clustering of dementia offers an alternative approach to identify susceptibility variants with higher penetrance. In this study, we summarize the identification and functional characterization of a rare *TREM2* coding variant associated with a familial form of dementia.

2 | MATERIAL AND METHODS

2.1 | Patients and controls

A nonconsanguineous family from Portugal affected by familial dementia was identified (Figure 1). The mother of the patient (II:2) was diagnosed with AD at age of 76 and her grandmother on the mother's side (I:2) also showed late-onset dementia. Only the index patient (III:1) of this family could be examined in more detail. Additional information on affected members in this family was obtained from accompanying healthy relatives. Diagnosis of probable AD in the index patient was assigned according to both National Institute of Neurological and Communicative Disorders and Stroke and the Alzheimer's Disease and Related Disorders Association (NINCDS/ADRDA) criteria (McKhann et al., 1984) and the core clinical of the National Institute on Aging-Alzheimer's Association (NIA-AA) criteria (McKhann et al., 2011). Consent was obtained from all participants. The studies were approved by the respective ethics committees. Genomic DNA was extracted from EDTA blood samples according to standard protocols. Screening of the identified *TREM2* variant was performed in Spanish and German AD cases and healthy controls.

The Spanish sample was recruited between 2003 and 2012 at the Memory Disorders Unit, Department of Neurology, Clínica Universidad de Navarra, School of Medicine (Pamplona, Spain; Benitez et al., 2013). Probable AD diagnoses were assigned according to both NINCDS/ADRDA criteria (McKhann et al., 1984), and the core clinical NIA-AA criteria (McKhann et al., 2011). Written informed consent was obtained from all participant of this study. The study was approved by the local Institutional Review Board. In this screening, 324 AD patients were included with an age at disease onset (AAO) of 74.1 ± 5.3 (mean ± standard deviation [*SD*]), 40% of patients were male. The control sample included 350 participants without cognitive deficits with a mean age at the latest assessment of 66.5 ± 11.5, 40% of controls were male.

In the German sample, all patients fulfilled NINCDS/ADRDA criteria for probable AD (McKhann et al., 1984). For the present screening, 940 AD samples were analyzed with 36% males and AAO of 72.1 ± 19.3. The patients with AD included in this study derived from the German Dementia Competence Network (Kornhuber et al., 2009), the German study on Aging, Cognition, and Dementia in primary care patients (AgeCoDe; Jessen et al., 2011), and the interdisciplinary Memory Clinic at the University Hospital of Bonn (Ramirez et al., 2014). Detailed description on inclusion criteria and diagnostic protocols for the AD cohort have been described elsewhere (Heilmann et al., 2015; Ramirez et al., 2014).

Control samples were obtained from the AgeCoDe cohort. Herein, AgeCoDe participants were included in the control group if they remain free of any cognitive impairment until the last visit. A total of 919 control samples were screened with 37% males and an age at last visit of 86.9 ± 3.2.

2.2 | Whole-exome sequencing

Whole-exome sequencing (WES) was performed in three members of the family after genomic DNA was isolated from EDTA blood samples. Enrichment of exonic and adjacent intronic sequences was performed with the NimbleGen Sequence Capture Human Exome 2.1M Array (Roche NimbleGen). Sequencing was performed on the Illumina Genome Analyzer IIx Sequencer (Illumina). The Varbank pipeline v2.1 and user interface, developed by the Cologne Center for Genomics, was used for the analysis and filtering of variants (https://varbank.ccg.uni-koeln.de). Herein, mean coverage was at least 68x in all three exomes (68×–81×), and ~90% of target bases were covered more than 20×. For the variant discovery analysis, the Genome Analysis Toolkit best practices recommendation were used as implemented in the VarBank interface (for details on the VarBank pipeline see [Kawalia et al., 2015] and [Alawbathani et al., 2018]). Numbering of variants in *TREM2* were done using the NCBI reference sequence NM_018965.3.

2.3 | Chemicals

The chemicals, used in this study, were purchased from following companies. Dulbecco's modified Eagle's medium (DMEM), penicillin–streptomycin (10.000 U/ml), Lipofectamine 2000, and Opti-MEM® for cell culture were purchased from Life Technologies. Fetal calf serum (FCS) was ordered from PAN-Biotech, (Germany) and Sigma-Aldrich; phosphate-buffered saline (PBS), EDTA, Endo H, and PNGase F glycosidases were from NEB; poly-L-lysine hydrobromide, NP-40 (IGEPAL® CA-630); glycerol were purchased from Sigma-Aldrich; and SDS pellets (sodium dodecyl sulfate) were gained from Roth, Germany. Sodium chloride, Tris, skimmed milk powder, glycine Tween® 20, and Triton X-100 were

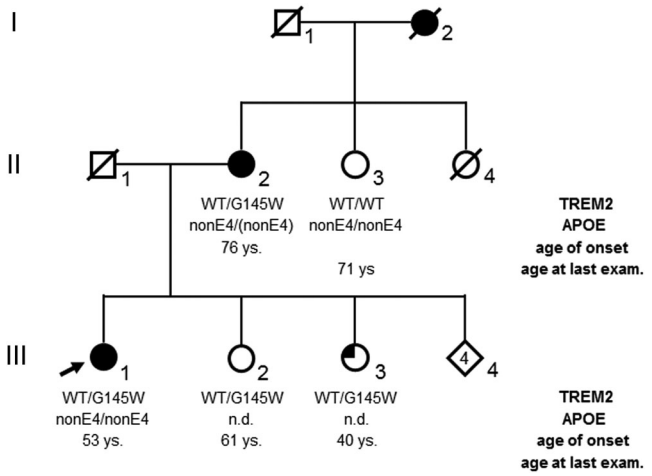

FIGURE 1 Pedigree of a family with early onset dementia. Affected family members are shown in black, a filled upper quadrant denotes subjective memory complaints. Further pedigree symbols are: circle, female; square, male; strikethrough, deceased; and rhomboid, additional siblings with no specified information. The index patient is marked by an arrow. Below the symbol, information about the carrier status of the identified *TREM2* variant, the APOE-ε4 genotype, as well as the age of disease onset for affected individuals or the age at last examination for unaffected family members is shown. The status of the second APOE-ε4 allele in II:2 is unsure due to low coverage in exome sequencing. One letter amino acid code was used for depicting TREM2 protein variants. WT, wildtype

purchased from AppliChem, Germany. Complete Mini protease inhibitor cocktail tablets were gained from Roche Applied Science, Germany. Bromophenol blue was used from Merck, Germany. EZ-Link Sulfo-NHS-Biotin and Pierce Streptavidin Agarose beads were purchased from Thermo Fisher Scientific, Germany.

2.4 | Primary and secondary antibodies

Following antibodies were used: goat anti-hTREM2 (#AF1828, 1:1,000 diluted) from R&D Systems; mouse anti-Flag M2 (#F1804, 1:1,000 diluted) and mouse anti-α-Tubulin antibody (#T5168, 1:1,000) from Sigma-Aldrich; mouse anti-c-Myc antibody (#2276, 1:1,000) from Cell Signaling Technology, secondary antimouse and antirabbit antibodies conjugated with horseradish peroxidase (#sc-2030 and #sc-2005, dilution 1:5,000) from Santa Cruz Biotechnology, Inc., secondary antibodies conjugated with IRDye® 680LT (#926–68022 and #926–68023, dilution 1:5,000) or IRDye® 800CW (#926–32212 and #926–32213, dilution 1:5,000) were purchased from LI-COR. Additional information of used antibodies is given in the corresponding figure legends.

2.5 | Cell lines

Human embryonic kidney cells HEK293 were purchased from CLS Cell Lines Service GmbH (Germany) and COS-7 cells obtained from DSMZ (German Collection of Microorganisms and Cell lines, Braunschweig, Germany). The cells were maintained at 37°C in a humidified atmosphere of 5% CO_2 in air in DMEM supplemented with 10% FCS and 1% penicillin–streptomycin (10.000 U/ml). COS-7 cells were maintained in DMEM with GlutamaxTM.

2.6 | DNA constructs

The DNAs encoding for human proteins were cloned into pcDNA^{TM}3.1(+) or pcDNA^{TM}3.1(−) and pEGFP-N1 expression vectors (#V790-20, Life Technologies). Open reading frames of the human TREM2 were cloned using primers attaching a DNA sequence encoding a c-Myc-tag to the 5′ ends and FLAG-tag or GFP (green fluorescent protein) to the 3′ ends, respectively, of the coding regions having the signal peptide in front of the N-terminal tag (Figure 2a). The FLAG tag was not present in c-Myc-TREM2-eGFP expression constructs (c-Myc-TREM2-eGFP). Variants NP_061838.1:p.(Gly145Trp), NP_061838.1:p.(Arg47His), NP_061838.1:p.(Thr66Met), NP_061838.1:p.(Gly145Ala), NP_061838.1:p.(Gly145Pro), NP_061838.1:p.(Gly145Ile), and NP_061838.1:p.(Gly145Phe) in TREM2 encoding DNA sequence were introduced by using QuikChange II Site-Directed Mutagenesis Kit (#200523, Agilent Technologies, Germany).

2.7 | Transfection of HEK293 cells

HEK293 cells were transfected with Lipofectamine 2000 (Life Technologies) according to manufacturer's protocol. After 24 hr, transfection cells were used for different experiments. Cells were cotransfected with plasmids encoding TREM2 and its coreceptor DAP12 to allow efficient subcellular transport of TREM2.

2.8 | Preparation of cellular membranes form HEK293 cells

Membrane fractions from transiently transfected HEK293 cells were prepared as described previously (Wunderlich et al., 2013). In brief, medium was aspirated and cells were washed once with ice-cold PBS about 24 hr after transfection. After washing HEK293 cells were incubated with hypotonic buffer (10 mM Tris, 1 mM EDTA, 1 mM EGTA in dH_2O, and pH 7.6) at 4°C under moderate shaking. Cell nuclei were separated from the homogenates by centrifugation at 300 *g* and 4°C for 10 min. Homogenates were again centrifuged at 16,000 *g* and 4°C for 60 min to separate cellular membranes from the cytosol. The pelleted membranes were lyzed by the addition of STEN lysis buffer and incubation on ice for 15 min. Membrane fractions were used for different biochemical analysis.

2.9 | Preparation of HEK293 cell lysates

For preparing cell lysates from transiently transfected HEK293 cells growth medium was aspirated and HEK293 cells were washed with ice-cold PBS (Dulbecco's phosphate-buffered saline, #D8537, Sigma-Aldrich). HEK293 cells were lyzed with DDM lysis buffer containing 0.2%

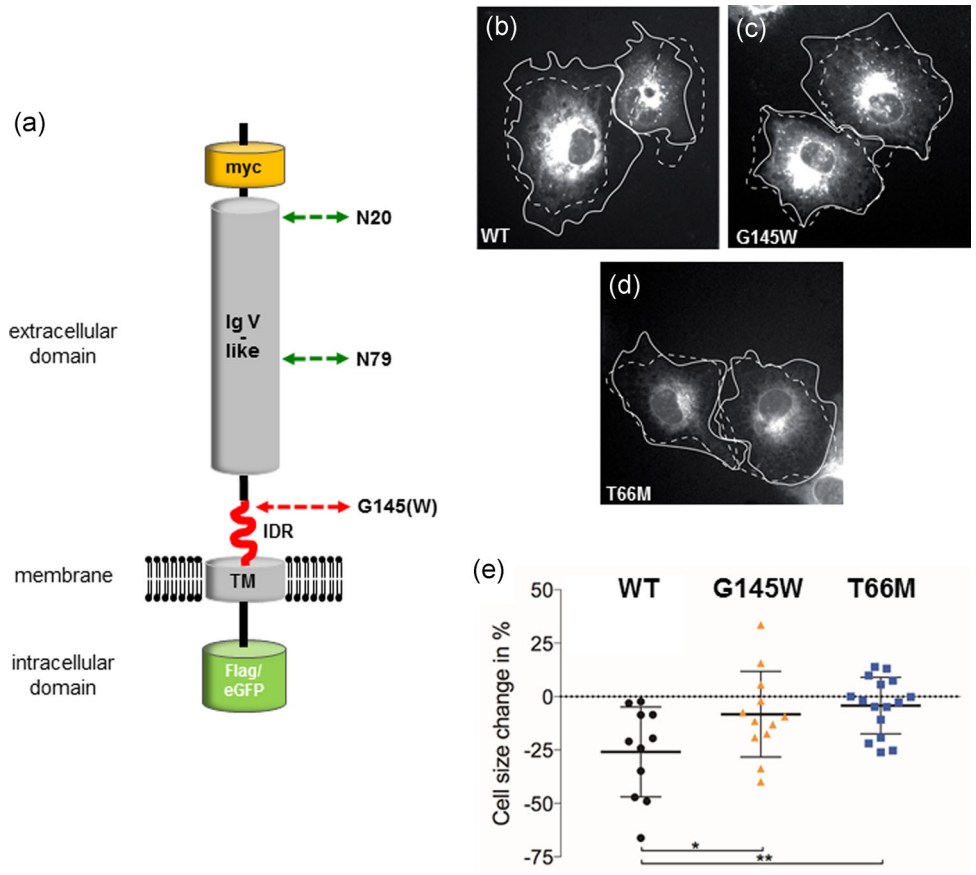

FIGURE 2 The p.(Gly145Trp) variant alters the morphological changes of TREM2-expressing cells. (a) Schematic drawing of the TREM2 with depicted functional domains, corresponding tags (Flag/GFP or myc) and the epitope binding region of the anti-TREM2-antibody. N-glycosylation sites are designated as N20 and N79, immunoglobulin-like domain as Ig_V-set domain, transmembrane domain as TM, intrinsically disordered region (IDR) is highlighted as a meandering line. Protein position glycine 145 with its variation to tryptophan is marked by an arrow (G145(W)). The N-terminal tag is located downstream of the signal peptide. (b–d) Representative fluorescent images of COS7 cells coexpressing $TREM2^{WT}$, $TREM2^{Gly145Trp}$, or $TREM2^{Thr66Met}$ with DAP12 upon 2 hr incubation with monoclonal antibody. A continuous line highlights the shape of the cell at the beginning of the experiment, dotted lines represent the cell shape at the end of the measurements. Changes in cell size were determined by subtraction of both areas. (e) Quantification of the cell size in different variants. Data are presented as means ± *SD* (−25.87 ± 21.06% for WT; −8.2 ± 20.09% for $TREM2^{Gly145Trp}$, and −4.22 ± 13.19% for $TREM2^{Thr66Met}$; $n = 5$ experiments, with 11–16 cells per condition in total. (*$p < ,05$; **$p < .01$). One letter amino acid code was used for depicting TREM2 protein variants. GFP; green fluorescent protein. WT, wildtype

DDM (n-Dodecyl β-D-maltoside, #D4641, Sigma-Aldrich), 150 mM NaCl (#A1149, AppliChem, Germany), 5 mM HEPES (pH 7.4, #A3268, AppliChem), 1 mM EDTA (pH 8.0, #E6635, Sigma-Aldrich), 10% glycerol (#15523, Sigma-Aldrich), 2 μM leupeptin hemisulfate (#CN33, Roth, Germany), 1 mM PMSF (in EtOH, #A0999, AppliChem), 20 mM NaF (#S7920, Sigma-Aldrich), 20 mM β-glycerophosphate (#A2253, AppliChem), and two Complete Mini protease inhibitor cocktail tablets (#04693124001, Roche Applied Science, Germany) in 50 ml dH_2O for 30 min at 4°C. Lyzed cells were transferred to 1.5 ml reaction vessel and centrifuged at 13,000 rpm and 4°C for 15 min. The supernatant corresponded with the HEK293 cell lysate and were used for expression analysis.

2.10 | Western blot analysis

Cell lysates were mixed with 6× Laemmli buffer (SDS loading buffer) containing 100 mM Tris-HCl (pH 6.8), 4% SDS, 60% glycerol, 0.2% bromophenol blue, and 10 mM dithiothreitol (DTT) in dH_2O. For preparation of urea gels 6 M urea was added to the gel buffer before polymerization as described previously (Prager et al., 2007). Proteins of the cell lysate were separated by SDS-PAGE (sodium dodecyl sulfate-polyacrylamide gel electrophoresis) as described previously (Nagler, Palkowitsch, Rading, Moepps, & Karsak, 2016). Briefly, protein extracts were transferred to Amersham Hybond enhanced chemiluminescence (ECL) nitrocellulose membrane (#RPN2032D, GE Healthcare, UK) and blocked with 5% skimmed milk powder in TBS-T (150 mM NaCl, 10 mM Tris, and 0.025% Tween® 20 in dH_2O). Primary antibodies in TBS-T or blocking buffer were incubated over night at 4°C, washed three times with TBS-T and incubated with secondary antibodies for 1 hr at room temperature. For visualization and detection of proteins the LICOR Odyssey® imaging system and the Pierce® ECL western blot analysis substrate (#32106, Thermo Fisher Scientific) were used.

2.11 | Digestion of membrane fractions by glycosidases

To investigate glycosylation pattern of TREM2 protein variants membrane fractions from HEK293 cells transfected with expression plasmids of WT and p.G145W TREM2 (signal peptide-Myc-hTREM2-FLAG) were digested with the glycosidases Endo H and PNGase F (NEB), respectively. Of note, glycosidase digestion was performed in a reaction end volume of 20 µl and due to the presence of 1% NP-40 in STEN lysis buffer used for the membrane fraction preparation, the addition of further NP-40 was not necessary. Membrane fractions were mixed with denaturation buffer and incubated at 100°C for 10 min. Afterwards glycosidases and corresponding reaction buffers were added, followed by incubation at 37°C for 1 hr. For control denatured membrane fraction with reaction buffers only was incubated. After glycosidase digestion membrane fractions were mixed with SDS loading buffer and analyzed by SDS-PAGE on 12% SDS separation gels and immunoblotting.

2.12 | Biotinylation of cell surface proteins

For biotinylation of cell surface proteins HEK293 cells were seeded on poly-L-lysine-coated 6-well plates (1×10^6 HEK293 cells per well). About 24 hr after seeding, HEK293 cells were transfected with Lipofectamine 2000 and Opti-MEM® according to manufacturer's protocol and kept for 24–32 hr at 37°C and 5% CO_2. Signal peptide-Myc-hTREM2-WT-FLAG or signal peptide-Myc-hTREM2-Gly145Trp-FLAG, respectively, were transfected together with hDAP12 plasmid. About 16 hr prior, biotinylation cells were washed briefly with PBS and conditioned medium was replaced by DMEM without FCS and antibiotics. To prevent internalization of cell surface proteins the following steps were performed on ice and with ice-cold solutions, respectively. First, cells were washed three times with ice-cold PBS. Then 2 ml of ice-cold and freshly prepared sulfo-NHS-biotin solution (c = 0.5 mg/ml in PBS) were added and cells were incubated for 30 min on ice under moderate shaking. To block unbound sulfo-NHS-biotin cells were washed for two times with ice-cold glycine solution (20 mM in PBS), followed by a third washing step with ice-cold glycine solution lasting 15 min on ice under moderate shaking. Afterwards cells were washed with ice-cold PBS and lysed by the addition of 400 µl STEN lysis buffer (150 mM NaCl, 50 mM Tris, 2 mM EDTA, 1% NP-40, 1% Triton X-100 in dH_2O, and pH 7.4) per well and incubation on ice for 15 min. Cell debris was removed by centrifugation at 12,000 g and 4°C for 10 min. To capture unbiotinylated proteins as a loading control, 20 µl of the samples were removed and prepared with 5 µl SDS loading buffer and stored at −20°C until SDS-PAGE. For biotinylation, 50 µl of washed streptavidin agarose slurry was added to cell lysates and incubated over night at 4°C by end-to-end rotation. Protein–agarose complexes were washed four times with STEN washing buffer (150 mM NaCl, 50 mM Tris, 2 mM EDTA, 0.2% NP-40, in dH_2O, and pH 7.6) by end-to-end rotation at 4°C for 10 min. Afterwards protein–agarose complexes were pelleted by centrifugation at 600 g and 4°C for 3 min. After washing procedure 25 µl SDS loading buffer (100 mM Tris-HCl [pH 6.8], 4% SDS, 60% glycerol, 0.2% bromophenol blue, and 10 mM DTT in dH_2O) was added and samples were incubated at 70°C for 10 min. Biotinylated protein precipitates and cell lysate controls were analyzed by SDS-PAGE on 12% SDS separation gels and immunoblotting. The images were quantified by Image J software (Schneider, Rasband, & Eliceiri, 2012).

2.13 | Cell morphology assay

COS-7 cells coexpressing human TREM2-GFP and DAP12 were seeded onto 35 mm µ-dishes (IBIDI, Germany) and changes in cell morphology were assessed as previously described (Glebov, Wunderlich, Karaca, & Walter, 2016). Briefly, 24–36 hr posttransfection COS-7 cells were monitored by fluorescence microscopy (ZEISS Axiovert 200M) for 10 min to determine spontaneous changes of the cell area. Thereafter, monoclonal anti-myc antibody (1 µg/ml) was added to the medium and imaging was continued for additional 2 hr. Changes in cell surface area were determined by subtracting the area after 2 hr of stimulation from that before stimulation. Images and measurements of the cell area were performed using ZEN Blue edition software (Zeiss, Germany). The specificity of the assay was confirmed with isotype control mouse monoclonal antibodies (6E10 against β-amyloid) as previously reported (Glebov et al., 2016). The $TREM2^{Thr66Met}$ served as a positive control. About 10–16 cells per condition were imaged.

2.14 | Statistical analysis

All data are presented as mean ± *SD*. Statistical comparisons among groups were performed by two-way analysis of variance (ANOVA) test. When comparing two groups, we used two-tailed Student's t tests. The $p \leq .05$ was considered statistically significant. Data from assay for cell morphology experiments were analyzed by one-way ANOVA with Dunnett ad hoc posttest. GraphPad Prism 7 (GraphPad software) was used for data analysis.

3 | RESULTS

3.1 | Whole-exome sequencing (WES) in a family with dementia revealed a rare coding variant in TREM2

In our neurology outpatient clinic, a patient consulted with symptoms compatible with a cognitive disease. This patient (III:1, Figure 1) was a 57-years-old female who initially presented symptoms of progressive cognitive decline at 53 years of age. The first symptoms comprised forgetfulness of recent conversations and difficulties to find things in a familial environment (e.g., at home). She was repetitive in conversations and easily forgot recent facts. One year after disease diagnosis the family reported language problems with difficulties of naming ordinary things. Two years after diagnosis, her activities of daily living declined progressively, requiring supervision

and becoming soon fully dependent on external help. Her relatives reported previous medical history of anxiety and a benign breast tumor. Neurological examination revealed nonfluent global aphasia, with anomia, semantic and phonemic paraphasia, and difficulties to understand orders of more than one item as well as imitatory apraxia. There was left hemineglect with difficulties to fix the gaze (optical ataxia). Mini-Mental (MMSE) score was 4/30 and severe cognitive impairment did not allow further neuropsychological assessment. There was no limb weakness. Muscular tone was normal and generalized hyperreflexia was observed. No myoclonus or other movement disorders were found. She could stand with no help but did not know were to go by herself without gestural indication. A brain MRI scan performed 2 years after disease onset in a different center (pictures not available) was reported to exhibit diffuse cortical atrophy. She was diagnosed with early-onset probable AD-type dementia (primary progressive aphasia which rapidly evolved towards posterior cortical atrophy syndrome). Exploring her family history revealed that her mother (II:2) was also diagnosed with probable AD dementia with subjective onset of memory impairment starting at the age of 76 years (Figure 1). At the last visit of the index patient, her mother was 88 years old and was reported to exhibit severe dementia according to her family relatives. No more medical information was available. Moreover, the deceased maternal grandmother of the index patient (I:2) was also reported to have had a dementia disease. In addition, a sister of the index patient, individual III:3 (Figure 1), reported subjective memory complaints starting at the age of 40 years, unfortunately we could not follow-up this individual in more detail.

The familial clustering of dementia led us to assume the existence of a genetic susceptibility variant with relatively high penetrance leading to dementia with a variable age at disease onset, which can manifest already at the age of around 50 years. The index patient in this family (III:1) was *APOE-ε4* negative and targeted sequencing revealed no variations in *PSEN1* (presenilin 1), *PSEN2* (presenilin 2), or *APP* (amyloid beta precursor protein). For this reason, we decided to search for underlying genetic variant(s) by performing WES (for more details see Material and Methods) in the DNA samples of both living affected family members (II:2 and III:1) and one member (II:3) who was cognitively healthy until the last visit at the age of 71 years, and, therefore, was operationally classified as healthy. Given the suspected mode of inheritance, we set up the bioinformatic filters to search for rare heterozygous variants (MAF < 0.02%) present in both affected members and not in the unaffected member of the family. We focussed our search on variants predicting protein truncation, splicing disturbances, and/or amino acid exchange.

In a first step, we analyzed the exome data for known monogenic disease genes involved in autosomal dominant forms of early onset dementia, however, no rare variants were identified in *APP*, *GRN* (granulin precursor), *MAPT* (microtubule associated protein tau), *PRNP* (prion protein), *PSEN1*, and *PSEN2*, although the coding part of these genes were sufficiently covered. Analyzing the exome data concerning the single nucleotide polymorphisms (SNPs) rs429358 and rs7412, that is, the two SNPs underlying the APOE-ε polymorphism, showed very low coverage for rs7412, which was probably due to the high GC content of this region. However, both III:1 and II:3 showed sufficient coverage for rs429358, which in fact defines the ε4 allele. Both were proven to be negative for the ε4 allele (i.e., "T/T"). For II:2, there was relatively low coverage for rs429358, which, however, also suggested the absence of the ε4 allele, although we cannot definitely exclude the presence of one ε4 allele. As to be expected for the subsequent exome-wide analytical step in a relatively small number of close relatives, we identified variants in around 65 different candidate genes. However, the genes carrying these rare variants had no obvious link to hereditary neurodegenerative dementias with one single exception, that is, a rare variant in exon 3 of *TREM2* (RefSeq NM_018965.3:c.433G>T/p.[Gly145Trp]). Finally, we did not detect potentially damaging rare variants fulfilling above mentioned criteria in *ABCA7*, *ABI3*, and *SORL1* for which previous reports identified damaging rare variants in sporadic and familial AD (Bellenguez et al., 2017; Sims et al., 2017).

We, therefore, focused our research on TREM2 p.(Gly145Trp). This variant predicts a substitution of glycine by tryptophan in the extracellular domain of TREM2 at amino acid position 145 and was predicted to be "probably damaging" (score of 0.988) by Polyphen-2 (http://genetics.bwh.harvard.edu/pph2/; assessed on July 17th, 2019) and to "affect protein function" (score of 0.02) by SIFT (https://sift.bii.a-star.edu.sg/sift-bin/SIFT_seq_submit2.pl; assessed on July 17th, 2019). It was neither found in 1,269 in-house controls nor in 1,403 sporadic AD patients of Spanish or German decent and was present only once (in an individual of European [non-Finnish descent] in 251,150 control alleles in the Genome Aggregation Database (gnomAD; https://gnomad.broadinstitute.org/). It is specifically not present in 34,570 alleles of individuals of the Latino population making it rather unlikely that it has a substantial frequency in the Spanish/Portuguese population. Interestingly, if restricting the gnomAD analysis to the so called "non-neuro" population (comprising 207,844 alleles) there is no occurrence of this variant, meaning that the single individual with the p.Gly145Trp variant in gnomAD has a neurological phenotype. This variant in *TREM2* was also identified in a heterozygous state in the putatively affected individual III:3 (Figure 1), however, also the as yet healthy family member III:2 (61 years of age) has this variant in a heterozygous state. Due to the known meaning of *TREM2* variants for different types of familial forms of dementias and the compatibility of the segregation of the variant with the clinical findings in the family (allowing for incomplete penetrance), we considered the p.(Gly145Trp) variant in *TREM2* as the prime candidate for disease susceptibility in this family, which was, therefore, further analyzed in biochemical and functional cellular studies. Notwithstanding, we cannot rule out that further variants in additional genes may also contribute to the increased disease susceptibility, which, however, was not the focus of this study.

3.2 | The p.(Gly145Trp) variant compromises TREM2 signaling activity

Ligand-induced activation of TREM2 results in Ca^{2+}-mediated rearrangement of the cytoskeleton accompanied by cell morphological changes (Glebov et al., 2016; Kiialainen et al., 2007; Peng et al., 2010). To compare the signaling activity of the novel $TREM2^{Gly145Trp}$ variant to that of the wildtype protein ($TREM2^{WT}$), we used N- and C-terminally tagged TREM2 constructs with c-Myc epitope and eGFP, respectively (c-Myc-TREM2-eGFP; Figure 2a). The c-Myc epitope tag served the purpose of specifically activate TREM2 by antibody cross-linking, whereas the eGFP signal was used to identify TREM2-expressing cells (Figure 2b; Glebov et al., 2016; Takahashi, Rochford, & Neumann, 2005; Wunderlich et al., 2013). Activation of the $TREM2^{WT}$ by anti-c-Myc antibody resulted in a time-dependent decrease in cell size (Figure 2b). Interestingly, cells expressing $TREM2^{Gly145Trp}$ presented significantly weaker responses upon activation with the anti-c-Myc antibody as compared with the $TREM2^{WT}$-expressing cells (Figure 2c). For further comparison, we tested a well-known loss-of-function mutant of TREM2, the p.(Thr66Met) variant. As expected, this variant also showed a significantly weakened cellular response following TREM2 activation by anti-c-Myc antibody (Figure 2d). The response of the $TREM2^{G145W}$-expressing cells resembled that of cells expressing $TREM2^{Thr66Met}$ suggesting that the p.Gly145Trp variant impairs signaling activity of TREM2 (Figure 2e).

3.3 | The p.(Gly145Trp) variant introduces structural changes in TREM2

The TREM2 variants were also expressed in HEK293 cells, and immunoblot analysis revealed a main band of ~28 kDa for the $TREM2^{WT}$ (Figure 3a). We noted that $TREM2^{Gly145Trp}$ variant migrated slightly faster in SDS-PAGE (with approx. 2 kDa lower apparent molecular mass) than $TREM2^{WT}$. The electrophoretic migration difference was absent in both additionally tested AD-associated TREM2 variants p.(Arg47His) and p.(Thr66Met; Figure 3a). This difference in gel mobility of p.(Gly145Trp) vanished upon addition of 6 M urea to the SDS gels (Figure 3b) suggesting that higher electrophoretic mobility of $TREM2^{Gly145Trp}$ likely resulted from conformational changes. This notion was further corroborated by immunoblotting with anti-Myc antibody recognizing the c-Myc epitope at the N-termini, and with anti-FLAG antibody directed towards a C-terminally fused FLAG tag of the tested TREM2 variants, thereby demonstrating that the differential migration was not a result of altered proteolytic processing (Figure 3a). The immunodetection by an anti-FLAG antibody also revealed a C-terminal fragment (CTF) of TREM2 at ~17 kDa for $TREM2^{WT}$, $TREM2^{Thr66Met}$, $TREM2^{Arg47His}$, and $TREM2^{Gly145Trp}$ variants (Figure 3a,b). Strikingly, a generic anti-TREM2 antibody raised against the human TREM2 ectodomain ranging from H19-S174 showed markedly reduced recognition of the $TREM2^{Gly145Trp}$ variant compared with $TREM2^{WT}$ (Figure 3a). This strong difference in intensities was neither observed with the antibody against the N-terminal c-Myc-tag nor the C-terminal FLAG-tag, further supporting a conformational effect of the p.(Gly145Trp) variant.

3.4 | p.(Gly145Trp) in TREM2 does not induce changes in membrane localization and glycosylation pattern

We next sought to explore whether the p.(Gly145Trp) variant affects expression and cell surface localization of TREM2 (Figure 4a). Transiently transfected HEK293 cells expressing $TREM2^{WT}$ or $TREM2^{Gly145Trp}$ were surface labeled with EZ-link^{TM} Sulfo-NHS-biotin. Quantification of immunoblot signals using the anti-TREM2 antibody revealed a reduced protein signal for $TREM2^{Gly145Trp}$ compared with $TREM2^{WT}$ in both cell lysate and biotinylated protein fraction (Figure 4a). However, for both variants the fraction of the protein at the cell surface was equal when normalized to the amount of TREM2 protein in the cell (Figure 4b), suggesting that both, mutant and WT, exhibited similar cellular trafficking efficiency.

The maturation process of TREM2 includes glycosylation (Kleinberger et al., 2014; Park et al., 2015; Wunderlich et al., 2013). We, therefore, tested whether the p.(Gly145Trp) variation affects TREM2 glycosylation that might also contribute to the differential migration pattern seen in SDS-PAGE. Membrane fractions of TREM2-expressing cells were treated with the N-glycosidases EndoH or PNGase F (Figure 4c). Treatment with EndoH or PNGase F resulted in faster migration of both $TREM2^{WT}$ and $TREM2^{Gly145Trp}$ at ~30 kDa instead of ~35 kDa in untreated samples (ctrl). The sensitivity of the main band at ~35 kDa to EndoH also indicates that this variant contains immature mannose-rich glycostructures. Interestingly, the altered gel mobility of $TREM2^{Gly145Trp}$ was still apparent upon deglycosylation indicating that the altered migration does not result from differences in the glycosylation pattern.

3.5 | The p.(Gly145Trp) variant shortens the intrinsically disordered region in TREM2

Finally, we explored the effect of amino acid exchanges at this position on TREM2 conformation. Sequence analysis of TREM2 using the Predictor of Natural Disordered Regions database (PONDR; www.pondr.com, version from Jan 12, 2007) classified the short sequence stretch connecting the Ig-like domain with the transmembrane region of TREM2 as an intrinsically disordered region (IDR). Interestingly, the IDR is predicted to start exactly at position 145 and to end at position 168 (Figure 5a). However, the predicted IDR in $TREM2^{Gly145Trp}$ is shortened by nine amino acids and only spans position 154–168.

Further in silico analysis showed that the length of the TREM2 IDR could be differentially influenced by the nature of the amino acid at position 145 with pronounced shortening of the IDR by large hydrophobic amino acid residues, while amino acids with smaller

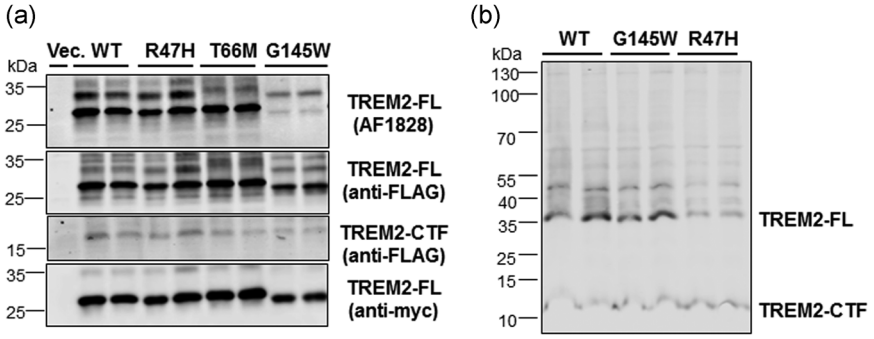

FIGURE 3 p.(Gly145Trp) influences the electrophoretic mobility of TREM2 in SDS-PAGE but not when denatured in 6 M urea. (a) and (b) Western blot images of protein lysates obtained from HEK293 cells expressing $TREM2^{WT}$ and $TREM2^{Gly145Trp}$ separated by (a) SDS-PAGE and (b) 6 M urea-SDS-PAGE and immunostained with different antibodies (given in brackets). $TREM2^{Thr66Met}$ and/or $TREM2^{Arg47His}$ were used as a control. Representative immunoblots from three comparable and independent experiments are shown. One letter amino acid code was used for depicting TREM2 protein variants. CTF, C-terminal fragment; FL, full length; IB, immunoblot; Vec., empty vector control; WT, wildtype

residues were predicted to have no or rather subtle effects on the length of the IDR (Figure 5b). To validate the effects of different amino acid substitutions on migration characteristics of TREM2 in SDS-PAGE, the respective TREM2 variants were expressed in HEK293 cells, and cell lysates subjected to immunoblot analysis. Interestingly, substitution of Gly145 by phenylalanine resulted in faster migration of TREM2 very similar to the p.(Gly145Trp) variant, suggesting that decreasing the length of the TREM2 IDR is responsible for the increased migration in SDS-PAGE. In contrast, substitution of Gly145 by alanine, predicted to have no effect on the length of the IDR, did not change migratory behavior of TREM2. Notably, the $TREM2^{Gly145Pro}$ variant, predicted to slightly enlongate the IDR, revealed slightly decreased migration, while the $TREM2^{Gly145Ile}$, predicted to slightly shorten the IDR also slightly increased migration in SDS-PAGE (Figure 5c). Thus, the glycine residue at position 145 is critical for the structure of the IDR in the TREM2 ectodomain. Together, the combined results indicate that the identified rare dementia-associated TREM2 variant p.(Gly145Trp) causes a conformational change of the IDR which could alter signaling characteristics upon activation.

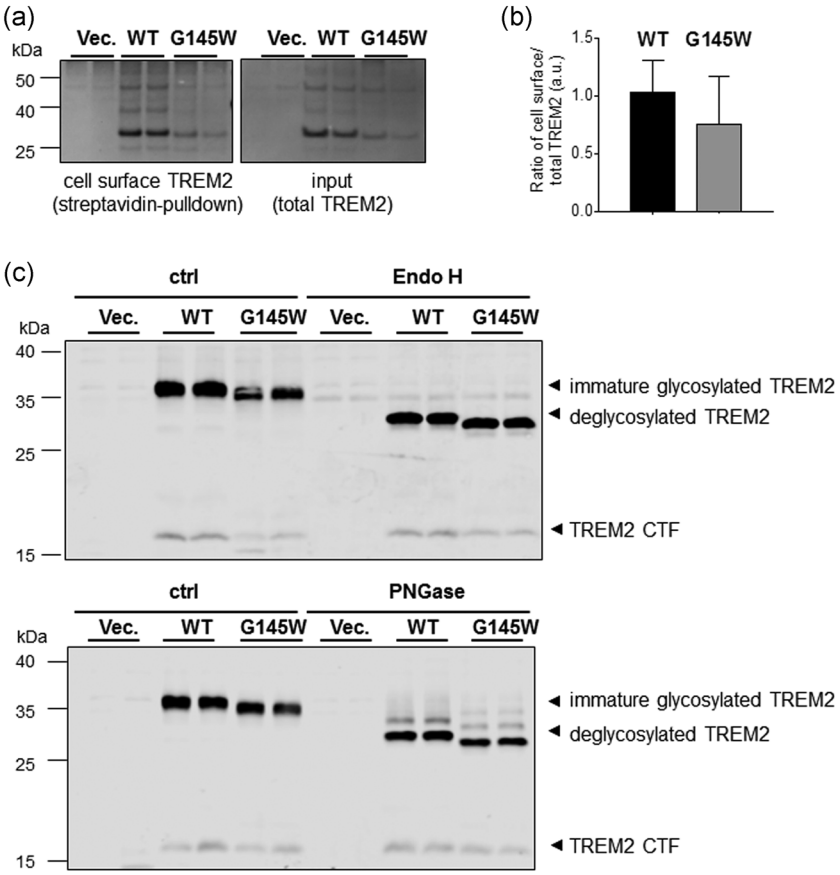

FIGURE 4 $TREM2^{Gly145Trp}$ exhibits a comparable membrane localization and glycosylation pattern to $TREM2^{WT}$. (a) Representative immunoblots of biotinylated HEK293 cells transfected with $TREM2^{WT}$ and $TREM2^{Gly145Trp}$. (b) Quantification of biotinylated TREM2 upon streptavidin pull down from the total TREM2 level. Data are means ± *SD* $n = 6$. (c) Immunoblot analysis of expression and glycosylation pattern of $TREM2^{WT}$ and $TREM2^{Gly145Trp}$ transfected in HEK293 cells using endoglycosidase H (EndoH) or PNGase F. One representative immunoblot from three independent experiments is shown. One letter amino acid code was used for depicting TREM2 protein variants. IB, immunoblot; Vec., empty vector control; WT, wildtype

(a)

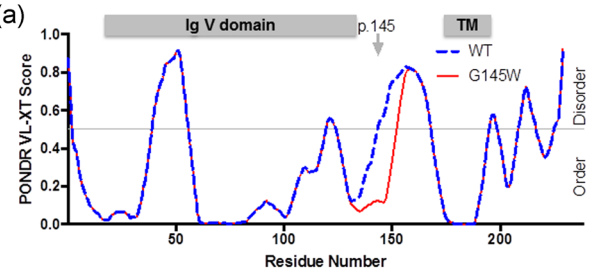

(b)

mut.	WT G145	G145W	G145P	G145A	G145I	G145F
aa		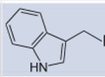				
IDR	145 - 168	154 - 168	143 - 168	145 - 168	148 - 168	152 - 168
length	23	14	25	23	20	16

(c)

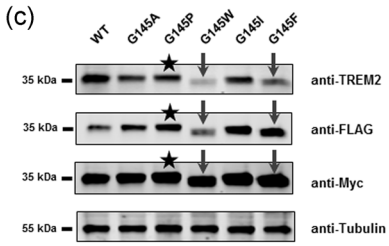

FIGURE 5 The p.(Gly145Trp) variant affects the length of the disordered region in TREM2. (a) Predictions of disordered regions of the VL-XT score (*V*ariously characterized *L*ong disordered regions and *X*-ray characterized *T*erminal disordered regions) using the PONDR®. The horizontal line represents the cutoff and values above the cutoff denote propensity for disorder. The dashed blue line represents values for $TREM2^{WT}$ and the continuous red line for $TREM2^{Gly145Trp}$. The position of the variation (p.[Gly145Trp]) and different TREM2 domains are designated. (b) In silico predictions for the length of the IDR (intrinsically disordered region) in other TREM2 variants containing different amino acid substitutions at position 145. (c) Representative immunoblots (n = 3) of TREM2 variants with substitution of G145. Variants ($TREM2^{Gly145Trp}$, $TREM2^{Gly145Phe}$, and $TREM2^{Gly145Pro}$) with distinct mobility in SDS-PAGE than the $TREM2^{WT}$ are designated by arrows (slightly increased migration) and by a star (slightly decreased migration). One letter amino acid code was used for depicting TREM2 protein variants. aa, amino acid; SDS-PAGE, sodium dodecyl sulfate-polyacrylamide gel electrophoresis; WT; wildtype

4 | DISCUSSION

Here, we describe a rare coding variant of *TREM2* which shows a segregation compatible with an incompletely penetrant probable AD-type dementia in a family showing familial clustering of dementia. The identified p.(Gly145Trp) substitution maps to the ectodomain of TREM2 and induces structural alterations leading to shortening of the IDR, which in turn decreases TREM2 signaling activity. In *TREM2*, the majority of identified pathogenic variations are located in the extracellular part of the protein (Yeh et al., 2017). Interestingly, the *TREM2* pathogenic variations involved in FTD-, FTD-like, and AD phenotypes, such as p.(Thr66Met), p.(Tyr38Cys), p.(Arg47His), p.(Val27Met), and p.(His157Tyr), seem to affect TREM2 function through different pathogenic effects at the protein level, including conformational changes in the ligand-binding domain (e.g., p.[Arg47His], p.[Thr66Met], and p.[Tyr38Cys]) and/or alter subcellular trafficking and glycosylation (e.g., p.[Thr66Met] and p.[Tyr38Cys]) or proteolytic shedding (e.g., p.[His157Tyr]) of TREM2 (Kleinberger et al., 2014; Sirkis et al., 2016). In contrast, the TREM2 p.(Gly145Trp) variant likely induces a conformational change of the IDR domain that connects the Ig-like and TM domain of TREM2 which impairs cellular response.

The glycine at position 145 of TREM2 sequence is located at the beginning of the IDR domain. Indeed, intrinsically disordered regions regularly show reduced binding of SDS thereby changing the electrophoretic mobility of the corresponding proteins (Receveur-Bréchot, Bourhis, Uversky, Canard, & Longhi, 2006; Uversky, 2009). The fact that $TREM2^{Gly145Trp}$ and $TREM2^{WT}$ migrated identically under strong denaturating conditions (i.e., 6 M urea-containing gels), further supports a conformational effect of the p.(Gly145Trp) substitution. Glycine is often found in IDRs (Habchi, Tompa, Longhi, & Uversky, 2014) and variations changing this amino acid might lead to a change in length of the IDR. Importantly, we observed that the length of the predicted disordered region correlates with the electrophoretic mobility of the mutant protein, that is, a decrease in IDR length results in higher mobility and vice versa. In line with these findings, we observed that exchanging the glycine at position 145 by alanine, does not change the mobility of TREM2. Conversely, other amino acids like phenylalanine or proline caused a shorting or enlargement of this IDR in TREM2, respectively, which is mirrored by a corresponding change in the electrophoretic mobility. Collectively, these results suggest that p.(Gly145Trp) induces conformational changes in the IDR that links the Ig-like domain and the transmembrane domain, which could contribute to the impaired signaling capacity of $TREM2^{Gly145Trp}$.

IDRs are dynamically disordered and can rapidly rearrange to different conformations creating the possibility to adapt and regulate cellular responses and signaling (Wright & Dyson, 2015). Dysfunctions of IDRs are often involved in neurodegenerative disorders, for example, linked to aggregation of amyloid-β peptide, tau-protein, and alpha-synuclein, each of which contains IDRs (Levine, Larini, LaPointe, Feinstein, & Shea, 2015; Uversky, 2009, 2015). So far, a variation within the IDR region p.(His157Tyr) has been previously identified to increase the shedding of TREM2 by α-secretase. This increased shedding leads to a reduction of full-length mature TREM2 at the cell surface that is able to bind ligands and trigger cellular signaling (Schlepckow et al., 2017). In contrast, biotinylation experiments showed similar expression of both $TREM2^{WT}$ and $TREM2^{Gly145Trp}$ at the cell surface. Thus, our findings support an additional pathogenic mechanism by which this amino acid variation in TREM2 might impair signal transduction, namely, by shortening and altering the flexibility of the IDR domain. In addition, IDRs play a central role in binding of ligands, or as "flexible entropic linkers" to separate functional protein domains (Wright & Dyson, 2015). Ligand binding might also induce conformational changes in

some IDRs which in turn modulates interactions with other partners (Wright & Dyson, 2015). In that regard it is noteworthy that the p.(Gly145Trp) substitution showed strongly decreased binding of a generic TREM2 antibody, indeed suggesting profound changes in the conformation of the TREM2 ectodomain, which might also mechanistically contribute to its pathogenicity.

The identification of an AD-associated variant in the IDR of TREM2 further stresses the importance of future research in the largely ill-defined role of IDRs in protein function and the possible involvement of genetic variants within IDRs for disease pathogenesis. From a human genetics point of view this seems especially noteworthy as common bioinformatic prediction tools may underestimate the functional consequences of variants within IDRs as compared to variants in well-structured and highly conserved protein domains with known functions.

Possible limitations of our study are related to the rather small size of the family and the variable onset of disease relatively late in adulthood. Besides the p.(Gly145Trp) variant, our filtering approach identified rare variants in more than 60 additional genes present in both affected family members and not present in the healthy family member, some of which might also contribute to the phenotype. Even more, the phenotype in this family might be additionally modulated by the cumulative effect (burden) of several common variants (MAF > 0.02%) clustered in the affected family member. It is also not known whether family member II:3, who does not bear the *TREM2* variant, or the healthy family member III:2, bearing the variant, will remain healthy or develop symptoms at an older age. Indeed, these kind of questions are typical for the genetic analysis of both monogenic and complex forms of disease disorders with onset in the adulthood, variable expressivity, incomplete penetrance, and large variability in disease onset. Nevertheless, the identified *TREM2* variant, which is extremely rare in the general population, does represent the most probable genetic susceptibility factor in the exome data set analyzed in this study. This conclusion is further supported by the profound alteration of protein structure and function observed in TREM2 carrying p.(Gly145Trp). Unfortunately, searching for genetic factors underlying the phenotype variability is nearly impossible with single families. Identification of these modifying factors has to be part of large international efforts analyzing the data of hundreds or even thousands of patients from families as the one presented in this study. From a clinical point of view, our results also show that next-generation sequencing-based diagnostic testing in familial forms of dementia should include the complete coding region of TREM2. The existence of heterozygous TREM2 variants with relatively large effect size furthermore emphasizes that pharmacological modification of TREM2 function may represent an attractive avenue for research with possible therapeutic implications for AD-type dementia.

In conclusion, our study provide evidence for a variant located in the IDR within the extracellular domain of TREM2 causing a loss of the TREM2 activation capability upon stimulation compared with $TREM2^{WT}$. This loss of function might mechanistically explain the clustering of dementia observed in the family. Furthermore, our study shows the functional relevance of the IDR domain for the ligand-induced signaling of TREM2. Further studies with other rare variants located in this region, if found, could provide additional information on the exact functional role of the IDR in TREM2.

ACKNOWLEDGMENTS

We thank all patients and controls for their participation in this project. This study was funded in part by the German Federal Ministry of Education and Research (grants KND: 01GI0102, 01GI0420, 01GI0422, 01GI0423, 01GI0429, 01GI0431, 01GI0433, and 01GI0434; grants KNDD: 01GI0710, 01GI0711, 01GI0712, 01GI0713, 01GI0714, 01GI0715, 01GI0716, and 01ET1006B). Part of this study was also funded by grants to Jochen Walter: DFG WA1477/6-2 (KFO177), Innovative Medicines Initiative 2 Joint Undertaking (IMI2 JU), grant/award number: No 115976 (PHAGO), and to KG (Alzheimer Forschung Initiative e.V. grant 16019). Center for Applied Medical Research, University of Navarra (CIMA; Pamplona, Spain) contributed to this study.

AUTHOR CONTRIBUTIONS

Study concept and design: M. K., J. W., and A. R.; Obtention of funding: M. K., J. W., A. R., M. T. H., F. J., A. S.-H., P. P., and W. M.; data acquisition and analysis: M. K., K. G., M. S., T. B., I. K., S. R., J. K., O. P., M. D.-F., L. F., M. H., J. Wi., M. Sch., S. R.-H., A. S., M. T. H., K. F., A. Sh., H. T., M. L., F. J., W. M., C. K., Z. I., P. N., P. P., J. W., and A. R.; Drafting the manuscript and figures: M. K., K. G., M. S., T. B., I. K., P. P., C. K., J. W., and A. R.; Review and editing the manuscript: all authors.

CONFLICT OF INTERESTS

The authors declare that there are no conflict of interests.

DATA AVAILABILITY STATEMENT

The data that support the findings of this study are available from the corresponding author upon reasonable request.

ORCID

Jochen Walter http://orcid.org/0000-0002-4678-2912
Alfredo Ramirez http://orcid.org/0000-0003-4991-763X

REFERENCES

Alawbathani, S., Kawalia, A., Karakaya, M., Altmüller, J., Nürnberg, P., & Cirak, S. (2018). Late diagnosis of a truncating *WISP3* mutation entails a severe phenotype of progressive pseudorheumatoid dysplasia. *Molecular Case Studies*, *4*(1), a002139. https://doi.org/10.1101/mcs.a002139

Bellenguez, C., Charbonnier, C., Grenier-Boley, B., Quenez, O., Le Guennec, K., Nicolas, G., … Jurici, S. (2017). Contribution to Alzheimer's disease risk of rare variants in TREM2, SORL1, and ABCA7 in 1779 cases and 1273 controls. *Neurobiology of Aging*, *59*, 220.e1–220.e9. https://doi.org/10.1016/j.neurobiolaging.2017.07.001

Benitez, B. A., Cooper, B., Pastor, P., Jin, S. C., Lorenzo, E., Cervantes, S., & Cruchaga, C. (2013). TREM2 is associated with the risk of Alzheimer's disease in Spanish population. *Neurobiology of Aging*, *34*(6), 1711.e15–1711.e17. https://doi.org/10.1016/j.neurobiolaging.2012.12.018

Gatz, M., Reynolds, C. A., Fratiglioni, L., Johansson, B., Mortimer, J. A., Berg, S., … Pedersen, N. L. (2006). Role of genes and environments for explaining Alzheimer disease. *Archives of General Psychiatry*, *63*(2), 168–174. https://doi.org/10.1001/archpsyc.63.2.168

Glebov, K., Wunderlich, P., Karaca, I., & Walter, J. (2016). Functional involvement of γ-secretase in signaling of the triggering receptor expressed on myeloid cells-2 (TREM2). *Journal of Neuroinflammation*, *13*, 17. https://doi.org/10.1186/s12974-016-0479-9

Guerreiro, R., Bilgic, B., Guven, G., Bras, J., Rohrer, J., Lohmann, E., … Emre, M. (2013). Novel compound heterozygous mutation in TREM2 found in a Turkish frontotemporal dementia-like family. *Neurobiol Aging*, *34*(12), 2890 e1-5. https://doi.org/10.1016/j.neurobiolaging.2013.06.005

Habchi, J., Tompa, P., Longhi, S., & Uversky, V. N. (2014). Introducing protein intrinsic disorder. *Chemical Reviews*, *114*(13), 6561–6588. https://doi.org/10.1021/cr400514h

Heilmann, S., Drichel, D., Clarimon, J., Fernández, V., Lacour, A., Wagner, H., … Ramirez, A. (2015). PLD3 in non-familial Alzheimer's disease. *Nature*, *520*(7545), E3–E5. https://doi.org/10.1038/nature14039

Jessen, F., Wiese, B., Bickel, H., Eiffländer-Gorfer, S., Fuchs, A., Kaduszkiewicz, H., … van den Bussche, H. (2011). Prediction of dementia in primary care patients. *PLOS One*, *6*(2), e16852. https://doi.org/10.1371/journal.pone.0016852

Jin, S. C., Benitez, B. A., Karch, C. M., Cooper, B., Skorupa, T., Carrell, D., … Cruchaga, C. (2014). Coding variants in TREM2 increase risk for Alzheimer's disease. *Human Molecular Genetics*, *23*(21), 5838–5846. https://doi.org/10.1093/hmg/ddu277

Karch, C. M., & Goate, A. M. (2015). Alzheimer's disease risk genes and mechanisms of disease pathogenesis. *Biological Psychiatry*, *77*(1), 43–51. https://doi.org/10.1016/j.biopsych.2014.05.006

Kawalia, A., Motameny, S., Wonczak, S., Thiele, H., Nieroda, L., Jabbari, K., … Nürnberg, P. (2015). Leveraging the power of high performance computing for next generation sequencing data analysis: Tricks and twists from a high throughput exome workflow. *PLOS One*, *10*(5):e0126321. https://doi.org/10.1371/journal.pone.0126321

Kiialainen, A., Hovanes, K., Paloneva, J., Kopra, O., & Peltonen, L. (2005). Dap12 and Trem2, molecules involved in innate immunity and neurodegeneration, are co-expressed in the CNS. *Neurobiology of Disease*, *18*(2), 314–322. https://doi.org/10.1016/j.nbd.2004.09.007

Kiialainen, A., Veckman, V., Saharinen, J., Paloneva, J., Gentile, M., Hakola, P., … Peltonen, L. (2007). Transcript profiles of dendritic cells of PLOSL patients link demyelinating CNS disorders with abnormalities in pathways of actin bundling and immune response. *Journal of Molecular Medicine*, *85*(9), 971–983. https://doi.org/10.1007/s00109-007-0191-4

Kleinberger, G., Yamanishi, Y., Suarez-Calvet, M., Czirr, E., Lohmann, E., Cuyvers, E., … Haass, C. (2014). TREM2 mutations implicated in neurodegeneration impair cell surface transport and phagocytosis. *Science Translational Medicine*, *6*(243), 243ra86. https://doi.org/10.1126/scitranslmed.3009093

Kornhuber, J., Schmidtke, K., Frolich, L., Perneczky, R., Wolf, S., Hampel, H., … Wiltfang, J. (2009). Early and differential diagnosis of dementia and mild cognitive impairment. *Dementia and Geriatric Cognitive Disorders*, *27*(5), 404–417. https://doi.org/10.1159/000210388

Krasemann, S., Madore, C., Cialic, R., Baufeld, C., Calcagno, N., El Fatimy, R., … Butovsky, O. (2017). The TREM2-APOE pathway drives the transcriptional phenotype of dysfunctional microglia in neurodegenerative diseases. *Immunity*, *47*(3), 566–581.e9. https://doi.org/10.1016/j.immuni.2017.08.008

Levine, Z. A., Larini, L., LaPointe, N. E., Feinstein, S. C., & Shea, J. -E. (2015). Regulation and aggregation of intrinsically disordered peptides. *Proceedings of the National Academy of Sciences*, *112*(9), 2758–2763. https://doi.org/10.1073/pnas.1418155112

Lill, C. M., Rengmark, A., Pihlstrøm, L., Fogh, I., Shatunov, A., Sleiman, P. M., … Bertram, L. (2015). The role of TREM2 R47H as a risk factor for Alzheimer's disease, frontotemporal lobar degeneration, amyotrophic lateral sclerosis, and Parkinson's disease. *Alzheimer's & Dementia*, *11*(12), 1407–1416. https://doi.org/10.1016/j.jalz.2014.12.009

McKhann, G., Drachman, D., Folstein, M., Katzman, R., Price, D., & Stadlan, E. M. (1984). Clinical diagnosis of Alzheimer's disease: Report of the NINCDS-ADRDA Work Group* under the auspices of Department of Health and Human Services Task Force on Alzheimer's Disease. *Neurology*, *34*(7), 939–939. http://www.ncbi.nlm.nih.gov/pubmed/6610841

McKhann, G. M., Knopman, D. S., Chertkow, H., Hyman, B. T., Jack, C. R., Kawas, C. H., & Phelps, C. H. (2011). The diagnosis of dementia due to Alzheimer's disease: Recommendations from the National Institute on Aging-Alzheimer's Association workgroups on diagnostic guidelines for Alzheimer's disease. *Alzheimer's & Dementia*, *7*(3), 263–269. https://doi.org/10.1016/J.JALZ.2011.03.005

Nagler, M., Palkowitsch, L., Rading, S., Moepps, B., & Karsak, M. (2016). Cannabinoid receptor 2 expression modulates Gβ1γ2 protein interaction with the activator of G protein signalling 2/dynein light chain protein Tctex-1. *Biochemical Pharmacology*, *99*, 60–72. https://doi.org/10.1016/J.BCP.2015.09.017

Paloneva, J., Mandelin, J., Kiialainen, A., Böhling, T., Prudlo, J., Hakola, P., … Peltonen, L. (2003). DAP12/TREM2 deficiency results in impaired osteoclast differentiation and osteoporotic features. *The Journal of Experimental Medicine*, *198*(4), 669–675. https://doi.org/10.1084/jem.20030027

Park, J. S., Ji, I. J., An, H. J., Kang, M. J., Kang, S. W., Kim, D. H., & Yoon, S. Y. (2015). Disease-associated mutations of TREM2 alter the processing of N-linked oligosaccharides in the Golgi apparatus. *Traffic*, *16*(5), 510–518. https://doi.org/10.1111/tra.12264

Peng, Q., Malhotra, S., Torchia, J. A., Kerr, W. G., Coggeshall, K. M., & Humphrey, M. B. (2010). TREM2- and DAP12-dependent activation of PI3K requires DAP10 and is inhibited by SHIP1. *Science Signaling*, *3*(122), ra38. https://doi.org/10.1126/scisignal.2000500

Poliani, P. L., Wang, Y., Fontana, E., Robinette, M. L., Yamanishi, Y., Gilfillan, S., & Colonna, M. (2015). TREM2 sustains microglial expansion during aging and response to demyelination. *Journal of Clinical Investigation*, *125*(5), 2161–2170. https://doi.org/10.1172/JCI77983

Prager, K., Wang-Eckhardt, L., Fluhrer, R., Killick, R., Barth, E., Hampel, H., … Walter, J. (2007). A structural switch of presenilin 1 by glycogen synthase kinase 3β-mediated phosphorylation regulates the interaction with β-catenin and its nuclear signaling. *Journal of Biological Chemistry*, *282*(19), 14083–14093. https://doi.org/10.1074/jbc.M608437200

Ramirez, A., van der Flier, W. M., Herold, C., Ramonet, D., Heilmann, S., Lewczuk, P., … Nöthen, M. M. (2014). SUCLG2 identified as both a determinator of CSF Aβ1–42 levels and an attenuator of cognitive decline in Alzheimer's disease. *Human Molecular Genetics*, *23*(24), 6644–6658. https://doi.org/10.1093/hmg/ddu372

Receveur-Bréchot, V., Bourhis, J. M., Uversky, V. N., Canard, B., & Longhi, S. (2006). Assessing protein disorder and induced folding. *Proteins: Structure, Function, and Bioinformatics*, *62*(1), 24–45. https://doi.org/10.1002/prot.20750

Schlepckow, K., Kleinberger, G., Fukumori, A., Feederle, R., Lichtenthaler, S. F., Steiner, H., & Haass, C. (2017). An Alzheimer-associated TREM2 variant occurs at the ADAM cleavage site and affects shedding and

phagocytic function. *EMBO Molecular Medicine*, *9*(10), 1356–1365. https://doi.org/10.15252/emmm.201707672

Schneider, C. A., Rasband, W. S., & Eliceiri, K. W. (2012). NIH Image to ImageJ: 25 years of image analysis. *Nature Methods*, *9*(7), 671–675. https://doi.org/10.1038/nmeth.2089

Shi, Y., & Holtzman, D. M. (2018). Interplay between innate immunity and Alzheimer disease: APOE and TREM2 in the spotlight. *Nature Reviews Immunology*, *18*(12), 759–772. https://doi.org/10.1038/s41577-018-0051-1

Sims, R., Van Der Lee, S. J., Naj, A. C., Bellenguez, C., Badarinarayan, N., Jakobsdottir, J., … Daniilidou, M. (2017). Rare coding variants in PLCG2, ABI3, and TREM2 implicate microglial-mediated innate immunity in Alzheimer's disease. *Nature Genetics*, *49*(9), 1373–1384. https://doi.org/10.1038/ng.3916

Sirkis, D. W., Bonham, L. W., Aparicio, R. E., Geier, E. G., Ramos, E. M., Wang, Q., … Yokoyama, J. S. (2016). Rare TREM2 variants associated with Alzheimer's disease display reduced cell surface expression. *Acta Neuropathologica Communications*, *4*(1), 98. https://doi.org/10.1186/s40478-016-0367-7

Takahashi, K., Rochford, C. D. P., & Neumann, H. (2005). Clearance of apoptotic neurons without inflammation by microglial triggering receptor expressed on myeloid cells-2. *The Journal of Experimental Medicine*, *201*(4), 647–657. https://doi.org/10.1084/jem.20041611

Ulland, T. K., & Colonna, M. (2018). TREM2 — a key player in microglial biology and Alzheimer disease. *Nature Reviews Neurology*, *14*, 667–675. https://doi.org/10.1038/s41582-018-0072-1. November 28. Nature Publishing Group.

Uversky, N. (2009). Intrinsic disorder in proteins associated with neurodegenerative diseases. *Frontiers in Bioscience*, *14*, 5188–5238. https://doi.org/10.2741/3594

Uversky, V. N. (2015). Intrinsically disordered proteins and their (disordered) proteomes in neurodegenerative disorders. *Frontiers in Aging Neuroscience*, *7*, 18. https://doi.org/10.3389/fnagi.2015.00018

Villegas-Llerena, C., Phillips, A., Garcia-Reitboeck, P., Hardy, J., & Pocock, J. M. (2016). Microglial genes regulating neuroinflammation in the progression of Alzheimer's disease. *Current Opinion in Neurobiology*, *36*, 74–81. https://doi.org/10.1016/j.conb.2015.10.004. February 1. Elsevier Current Trends.

Walter, J. (2016). The triggering receptor expressed on myeloid cells 2: A Molecular link of neuroinflammation and neurodegenerative diseases. *Journal of Biological Chemistry*, *291*, 4334–4341. https://doi.org/10.1074/jbc.R115.704981. February 26. American Society for Biochemistry and Molecular Biology.

Wright, P. E., & Dyson, H. J. (2015). Intrinsically disordered proteins in cellular signalling and regulation. *Nature Reviews Molecular Cell Biology*, *16*(1), 18–29. https://doi.org/10.1038/nrm3920

Wunderlich, P., Glebov, K., Kemmerling, N., Tien, N. T., Neumann, H., & Walter, J. (2013). Sequential proteolytic processing of the triggering receptor expressed on myeloid cells-2 (TREM2) protein by ectodomain shedding and γ-secretase-dependent intramembranous cleavage. *Journal of Biological Chemistry*, *288*(46), 33027–33036. https://doi.org/10.1074/jbc.M113.517540

Yeh, F. L., Hansen, D. V., & Sheng, M. (2017). TREM2, microglia, and neurodegenerative diseases. *Trends in Molecular Medicine*, *23*(6), 512–533. https://doi.org/10.1016/J.MOLMED.2017.03.008

How to cite this article: Karsak M, Glebov K, Scheffold M, et al. A rare heterozygous *TREM2* coding variant identified in familial clustering of dementia affects an intrinsically disordered protein region and function of TREM2. *Human Mutation*. 2019;1–13. https://doi.org/10.1002/humu.23904